Increased Fragmentation Efficiency of Ions in a Low Pressure Linear Ion Trap with an Added dc Octopole Field

B. A. Collings
MDS SCIEX, Concord, Ontario, Canada

In-trap fragmentation of ions in a hybrid linear ion trap triple quadrupole mass spectrometer occurs at pressures about 5e-5 torr. At these low pressures, efficient fragmentation of heavy ions (such as the singly charged homogenously substituted triazatriphosphorine of mass 2721.89 Da) can take a long time because of the relatively low collision frequency with the background gas and the high internal energy content required to produce fragmentation. Increasing the amplitude used for dipolar excitation leads to loss of the ion upon the quadrupole rods. In the work presented here, the addition of a dc octopolar field to a linear ion trap is described. The dc octopolar field was created by the addition of four auxiliary electrodes situated between the quadrupole rods at a distance of 10 mm from the axis. The inclusion of the dc octopolar field was shown to cause the ions' frequency of motion to shift out of phase with the excitation signal at high radial amplitudes. This resulted in beat-like trajectories with periods of excitation and de-excitation as the ions' frequency of motion shifted in and out of phase with the excitation signal. This led to a reduction in the loss of ions on the quadrupole rods during the excitation process. The result is an increased fragmentation efficiency relative to the fragmentation efficiency obtained when using an LIT constructed of round rods only. The inclusion of the dc octopolar field allowed the ion to be fragmented more efficiently in a relatively short excitation period. (J Am Soc Mass Spectrom 2005, 16, 1342–1352) © 2005 American Society for Mass Spectrometry

The fragmentation of ions at pressures about 5e-5 torr, in a low-pressure linear ion trap (LIT), requires the use of low excitation amplitudes and extended excitation periods [1, 2]. Pressures in this range are typical in the operation of hybrid linear ion trap triple quadrupole mass spectrometers that utilize the final quadrupole as both a mass resolving quadrupole and as a linear ion trap [3]. In this pressure regime, excitation amplitudes are limited from a few tens of millivolts to a few hundred of millivolts to prevent the ion from colliding with a quadrupole rod. It is the presence of the higher order field components [4–6] attributable to the use of circular rods, which enable the excitation to be carried out for extended periods of time without loss of the parent ion. A general expression for a two-dimensional multipole field can be written as

$$\Phi(x,y) = \sum_{n=0}^{\infty} \varphi_n(x,y) = \sum_{n=0}^{\infty} A_n \,\mathrm{Re}\left(\frac{x+iy}{r_0}\right)^n \qquad (1)$$

where $2n$ is the number of poles in a particular term. For example, A_2 is the amplitude of the quadrupole contribution with the higher order terms arising from $n > 2$. In the work presented here, the experimental ratio of the rod diameter to the field radius (r/r_0) was 1.126. It has been previously shown that the coefficients obtained from this ratio are $A_2 = 1.001462$, $A_6 = 0.001292$, $A_{10} = -0.002431$, and $A_{14} = -0.0002975$ with all other terms for which $n < 14$ equal to zero [4]. As the ion is excited to higher radial amplitudes, the ions' motion shifts out of phase with the excitation signal attributable to the presence of terms with $n > 2$. This results in the ion trajectory taking on a bead-like pattern and remaining stable within the radial trapping potential [1, 2]. For small ions, high fragmentation efficiencies approaching 100% can be achieved in less than 50 ms when fragmented at low q. Large ions may require several hundred milliseconds of excitation to achieve modest fragmentation efficiencies [1]. This is due to the increased number of collisions required to impart enough kinetic energy into the ion to cause fragmentation. Increasing the excitation amplitude results in increased loss of the ions upon the quadrupole rods. One significant drawback to using extended excitation periods is the decrease in overall scan duty cycle, an undesirable effect.

To decrease the excitation period, a number of possibilities exist. The pressure can be increased to allow for more collisions with the ion, the excitation q can be increased, or higher order fields can be superposed with

Published online June 24, 2005

Address reprint requests to Dr. B. Collings, MDS SCIEX, 71 Four Valley Drive, Concord, Ontario L4K 4V8, Canada. E-mail: bruce.collings@sciex.com

1044-0305/05/$30.00
doi:10.1016/j.jasms.2005.03.049

Received February 7, 2005
Revised March 28, 2005
Accepted March 29, 2005

the radial trapping potential. Increasing the static pressure in a hybrid LIT triple quadrupole is not feasible because the LIT doubles as the final analyzing quadrupole and is located in the same vacuum region as the ion detector. There is an upper pressure limit in this region that exists to prevent excessive ion feedback noise and long-term damage to the detector. The excitation q can be increased but with the resulting loss in mass range attributable to the low mass cut-off at $q = 0.907$. Increasing the content of the higher order fields allows increased fragmentation efficiencies without sacrificing mass range. Increasing the higher order field content beyond that which is normally present within the round rod quadrupole helps to further reduce loss of the ions to the rods during the excitation process at the higher radial amplitudes. The larger the content of the higher order field the more strongly dependent the ions' frequency of motion is upon its radial amplitude [2].

Higher order fields are routinely utilized in commercial 3-D ion traps [7]. In these devices, the fields are adjusted by altering the shape or position of the electrodes, which determines the content of the higher order fields [8, 9]. In general, the fields are adjusted to allow the ions to be ejected more rapidly from the ion trap than is otherwise possible in a 3-D quadrupole ion trap consisting of a purely quadrupolar trapping potential [7, 9]. The result is improved mass resolution when the ions are scanned out of the 3-D trap. Franzen and Wang have devised a 3-D quadrupole ion trap in which the higher multipole field fractions can be switched on and off [10, 11]. In this device the end cap electrodes are constructed of more than one section, allowing the content of the higher multipole fields to be varied. With the appropriate field content an ion can be fragmented more efficiently without loss of the parent ion.

In the work presented here, a set of four auxiliary electrodes were placed along the length of the LIT between the quadrupole rods at a distance of 10 mm from the axis of the quadrupole. The effects of the auxiliary electrodes upon the analyzing capabilities of the quadrupole, when operated in the normal mass analyzing manner, are minimized by appropriately adjusting the potentials on the auxiliary electrodes [12]. A dc potential applied to the auxiliary electrodes modified the radial trapping potential by the addition of a dc octopolar field. The addition of the dc octopolar field reduced the loss of the ions to the quadrupole rods during the excitation process, leading to an increase in fragmentation efficiencies. Through experiments and modeling, the frequency shifts and the increase in fragmentation efficiency as a function of the applied potential to the auxiliary electrodes are examined.

Experimental

Experimental Set-Up

Experiments were carried out on a modified 4000 Q TRAP® (AB/MDS Sciex, Concord, Ontario, Canada), a hybrid triple quadrupole linear ion trap mass spectrometer. The collision cell (Q2) contained typically 5 to 10 mTorr of nitrogen. The collision cell was modified to allow the axial field to be provided by a set of electrodes placed around the quadrupole rods [13]. The potential applied to these electrodes could be varied to give control over the magnitude of the axial field. The second analyzing quadrupole (Q3) performed the function of the linear ion trap (LIT) when operated in trap mode and was operated at a pressure of 3.5e-5 torr of nitrogen [1]. Each of the mass analyzing quadrupoles was 200 mm long with a field radius of 4.17 mm. The quadrupoles were operated at a drive frequency of 816 kHz. When operated in trap mode, the ions were scanned out of the LIT at 1000 Da/s using the technique of mass selective axial ejection [14] using a frequency of 312 kHz for the ejection signal. Two different styles of LIT were used for the experiments described below. In one set of experiments, the Q3 quadrupole was modified by adding four 200 mm long auxiliary electrodes along the length of the quadrupole. In another set of experiments, the auxiliary electrodes were removed. The auxiliary electrodes each had a 2 mm long stem along the length of the electrode that was positioned 10 mm from the central axis of the quadrupole as shown in Figure 1. A dc potential difference ranging from −220 V to +220 V was applied to the auxiliary electrodes relative to the Q3 quadrupole rod offset. Resonant excitation of the ions was accomplished using dipolar excitation applied between the A-pole rods of the quadrupole [1]. Experiments were carried out with q values ranging from $q \approx 0.205$ to $q \approx 0.3$. At these q values, the fundamental frequency of the ions' motion ranges from 60 to 88 kHz. The amplitude and duration of the excitation ranged from 0 to 343 mV and 100 ms, respectively, depending upon the experiment.

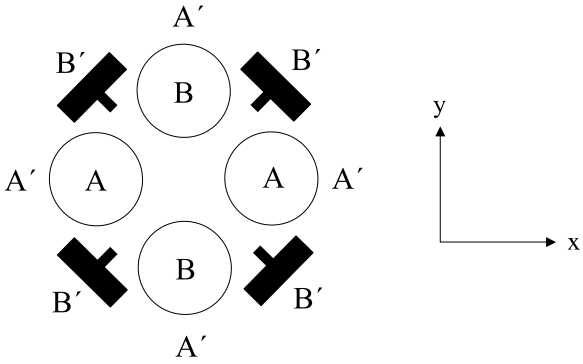

Figure 1. The electrode geometry used to create the dc octopole field. The A and B poles are the normal quadrupole rods. The letters A′ and B′ represent the positions of the A and B poles for the octopole. Applying a dc potential to the "T"-shaped electrodes creates the dc octopolar field.

The ion chosen for this study was a singly charged homogenously substituted triazatriphosphorine of mass 2721.89 Da [15]. The ion was obtained from a 1/10 dilution of an Agilent electrospray tuning solution (Agilent ES tuning mix, G2421, Palo Alto, CA). Trap fill

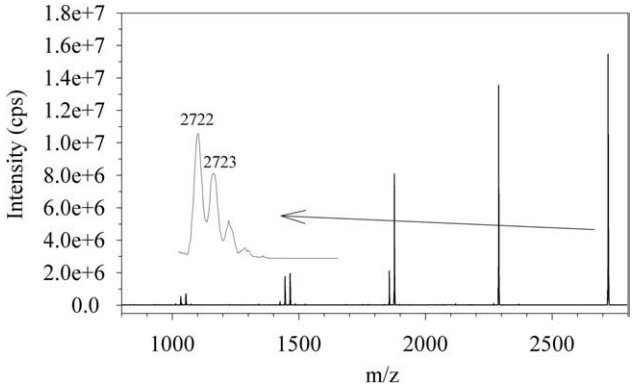

Figure 2. Fragmentation pattern observed for excitation of m/z = 2722 Th at 59.580 kHz. The excitation period was 100 ms, excitation amplitude was 255 mV_{0-p} and the excitation q was ~0.205. The auxiliary electrodes were held at +220 V relative to the quadrupole dc potential offset.

times were typically 50 ms with 25 scans co-added to produce each mass spectrum. Excitation of the isotopic cluster, at nominally m/z = 2722 Th, produced fragments down to ~1000 Th, Figure 2.

High-energy fragmentation spectra were collected using collision assisted dissociation (CAD). Mass spectra were collected using the EPI (enhanced product ion) mode in which the product ions are collected in the LIT before mass analysis.

Excitation of m/z = 2722 Th at $q \approx 0.205$ and $q \approx 0.3$ results in low mass cut-offs of 615 and 900 Da, respectively. Frequency response profiles were constructed by integrating the areas of the fragment ions and the parent isotopic cluster as a function of excitation frequency. This allowed determination of the resonant frequency of the ion as a function of the applied dc potential difference between the auxiliary electrodes and the quadrupole rods.

Ion Trajectory Simulations

Ion trajectory simulations were carried out to examine two different aspects of the excitation process. The first was to determine how many collisions the ion m/z = 2722 Th would suffer and how much center of mass collision energy was available for internal excitation during a 100 ms excitation period. The second aspect was to determine what effect the polarity of the auxiliary electrodes had upon the ion during the excitation process. In one set of simulations, a total of 100 ion trajectories were run using the simulator described in reference [11] with an electrode geometry corresponding to a normal round rod analyzing quadrupole. The ions were given random starting coordinates within a 1 mm radius of the quadrupole axis. The ions were then cooled at a pressure of 1 mTorr of nitrogen for a 5 ms period before excitation. The ions were excited using dipolar excitation with an amplitude of 80 mV and at frequency of 59,660 Hz (q = 0.205; 816 kHz drive frequency). The mass of the ion was 2722 Da and had a collision cross-section of 500 Å^2. The pressure during the simulation was 3.5e-5 torr of nitrogen. The resonance position was found by running several ion trajectories over a range of excitation frequencies and excitation amplitudes while monitoring the duration of each trajectory. The resonance was identified by those frequencies that stopped before the maximum allowed duration, i.e., the trajectory terminated on a rod surface. The collision cross-section of this ion with nitrogen was measured using the energy loss technique described by Covey and Douglas [16].

Modeling of the potential energy surfaces with various dc potentials applied to the auxiliary electrodes was accomplished through the use of the ion trajectory simulation program Simion 7.0 [17]. Simion 7.0 was used instead of the simulator described in reference [11] because of a limitation in the available electrode geometry of the in-house simulator at the time that this work was undertaken. The array shown in Figure 1 was modeled with an additional grounding cylinder placed at a distance of 6 r_0 around the quadrupole. The array was constructed using a 2000 × 2000 array with a resolution of 40 grid units/mm. This produced r_0 = 4.149 mm which is slightly less than the experimental r_0. To produce a more realistic r_0 would have required more RAM than was currently available on the workstation used at the time of the simulations.

Ion trajectories using m/z = 2722 Th were run on this array using dc potential differences ranging from −360 to +360 V between the auxiliary electrodes and the quadrupole rods. An rf amplitude of 660.9 V was applied to the quadrupole rods with a phase shift of 180 degrees between the A and B poles. This corresponded to $q \approx 0.205$. In one set of experiments the ions' frequency of motion was measured and plotted as a function of maximum radial amplitude attained during the simulation. In these experiments the ion was started at various radial amplitudes along the line x = 0. The ion was given zero initial kinetic energy, no collisions were allowed and the trajectories were allowed to run for 25 ms. Data were collected for the time and position of the ion at 1 μs intervals and then fast-Fourier-transformed to obtain the ions' fundamental frequency of motion. In another set of experiments, designed to study the effects of a positive versus negative dc potential applied to the auxiliary electrodes, the ion was started at a low radial amplitude and dipolar excitation was applied across the A pole rods. The trajectories in those experiments were allowed to run for a maximum of 25 ms or until the ion crashed into a rod. The ion trajectory was then examined to study the difference that the polarity of the applied potential had upon the ion trajectory.

Results and Discussion

CAD Experiments

Fragmentation of the ion m/z = 2722 Da, using collision assisted dissociation (CAD) in the Q2 gas cell, required fairly high collision energies with very little fragmenta-

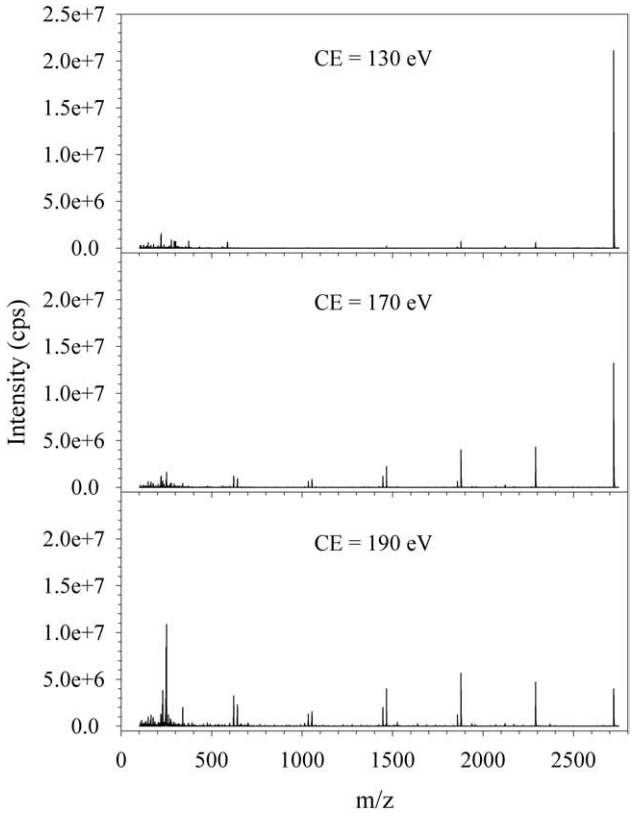

Figure 3. This figure shows the enhanced product ion spectra obtained for the ion m/z = 2722 Th at collision energies of 130, 170, and 190 eV with nitrogen in the Q2 collision cell. There is very little fragmentation observed at the lowest collision energy of 130 eV.

tion occurring at a collision energy of 130 eV. Mass spectra covering the mass range 100 to 2750 Da are shown for collision energies of 130, 170, and 190 eV in Figure 3. At collision energies of 170 and 190 eV there is a significant amount fragmentation.

Resonant Excitation Experiments

In one set of experiments data were collected without the auxiliary electrodes in place around the quadrupole. Figure 4 shows the degree of fragmentation and ion loss as a function of excitation amplitude obtained at $q \approx 0.205$ and $q \approx 0.3$ for a 100 ms excitation period. The increase in q resulted in an increase in maximum fragmentation efficiency from 10 to 35%. The increase in q provides a deeper pseudo-potential well that helps keep the parent and fragment ions in the LIT during the excitation process. The pseudo-potential well depth, $\bar{D}$, is described by [18].

$$\bar{D} = q\frac{V_{rf}}{4} \quad (2)$$

Using $q \approx 0.205$, m/z = 2722 Da, and V_{rf} = 660.9 V gives $\bar{D}$ = 33.9 V. Increasing q to 0.3 leads to an increase in V_{rf} to 967 V giving $\bar{D}$ = 72.5 V, a significantly deeper pseudo-potential well.

An alternative method for increasing fragmentation efficiency is to modify or add higher order field components to the trapping potential. The addition of auxiliary electrodes, as shown in Figure 1, produces a dc octopolar field. In an octopolar field the ions frequency of motion is dependent upon its radial amplitude. As the ion is excited to higher radial amplitudes its motion shifts out of phase with the excitation frequency. The ion takes on a complicated beat-like trajectory that can be sustained for extended periods of time without the ion crashing upon a quadrupole rod. Increasing the content of the dc octopolar field results in the ion going out of phase with the excitation frequency at even lower radial amplitudes. Higher excitation amplitudes are then required to bring the ion back to high radial amplitudes. It is the high radial amplitudes that provide high kinetic energies through the ions' micromotion, giving high center-of-mass collision energies. The presence of the dc octopolar field helps to reduce the loss of ions at the high radial amplitudes. The combination of the high kinetic energy and the reduced loss at high radial amplitudes allows for an increased level of internal excitation and fragmentation efficiency without changing the duration of the excitation period. This is demonstrated in Figure 5, where the percent fragmentation efficiency is plotted as a function of excitation amplitude. In this experiment, the auxiliary electrodes were held at +220 V relative to the

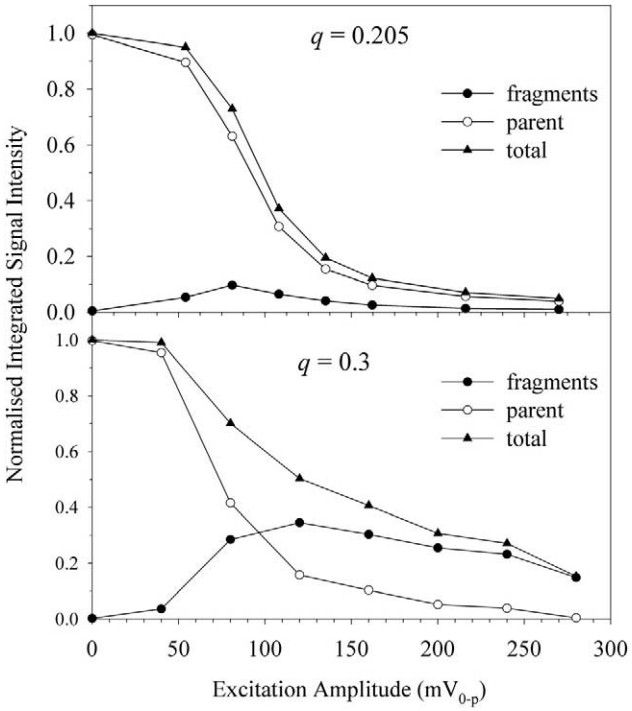

Figure 4. Normalized integrated signal intensity as a function of excitation q and excitation amplitude for a LIT without the presence of the auxiliary electrodes. The excitation period was 100 ms in both cases.

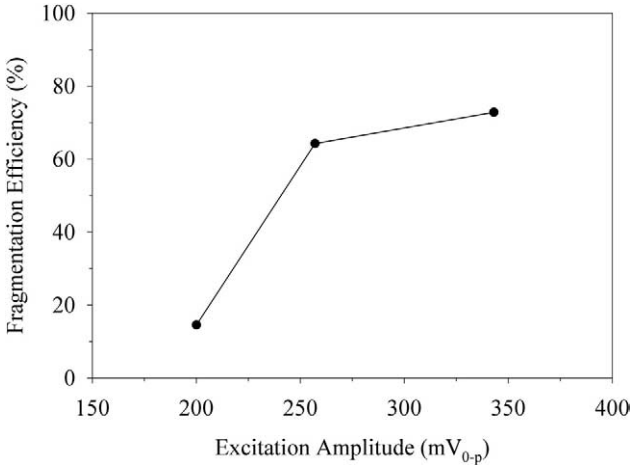

Figure 5. Percent fragmentation efficiency, at the maximum of the frequency response curve, as a function of excitation amplitude. The potential difference between the auxiliary electrodes and the quadrupole rods was constant at +220 V.

quadrupole rods. When the excitation amplitude was increased from 200 to 345 $mV_{0\text{-}p}$, the maximum of the frequency response profile shifted from 59.43 to 59.34 kHz. The excitation period was held constant at 100 ms.

The increases in fragmentation efficiency are also dependent upon the polarity of the dc octopolar field that is applied. It is not sufficient to simply phase-shift the ions' motion relative to the excitation signal. Experiments show that it is also necessary to apply the dc octopolar field with the same polarity as the ion of interest. Applying a negative potential difference to the auxiliary electrodes results in almost complete loss of the positively charged parent ion, whereas at the same excitation amplitude a positive potential difference leads to a high degree of fragmentation. This is shown in Figure 6, where the frequency dependence of the response profiles as a function of the applied potential difference to the auxiliary electrodes are plotted. The data were obtained using an excitation amplitude of 255 mV for each experiment. The first significant feature was a shifting of the ions' resonant frequency downwards as the potential on the auxiliary electrodes becomes more positive. The frequency decreases by ≈600 Hz when the applied potential difference was changed from −120 V to +220 V. With the exception of the data for a zero potential difference, the resonant frequency profiles have a FWHM of about 150 to 190 Hz. This width is sufficient to cover several isotopes, at the nominal *m/z* of 2722 Th, which are spaced by ~22 Hz [1]. Exciting the entire isotopic cluster instead of a single isotope will lead to a broadening of the frequency response profile by a few tens of Hz. Figure 7 shows a plot of the resonant frequency as a function of the potential applied to the auxiliary electrodes. Additional data have been included for excitation amplitudes ranging from 100 to 345 mV when the auxiliary electrodes were present, and ranging from 40 to 110 mV when they were absent. The data collected with no auxiliary electrodes were obtained with lower excitation amplitudes where the resonance width was about 150 Hz. It should be noted that the data acquired with no auxiliary electrodes is offset by +20 V for clarity. The data show approximately that the resonant frequency decreased linearly as the potential applied to the auxiliary electrodes was increased.

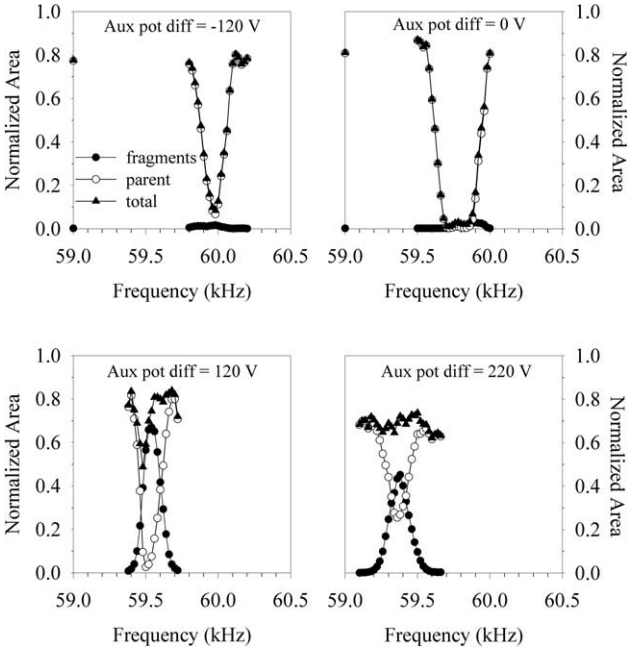

Figure 6. Frequency response profiles for *m/z* = 2722 Th as a function of potential difference between the quadrupole rod dc offset and the dc potential applied to the auxiliary electrodes. The excitation amplitude of 255 $mV_{0\text{-}p}$ was applied for a period of 100 ms in each experiment. The solid circles represent the integrated intensity of the fragment ions, the open circles the parent ion cluster, and the solid triangles the total or sum of the fragment and parent ions.

Further investigation revealed that the resonant frequencies were dependent upon the excitation ampli-

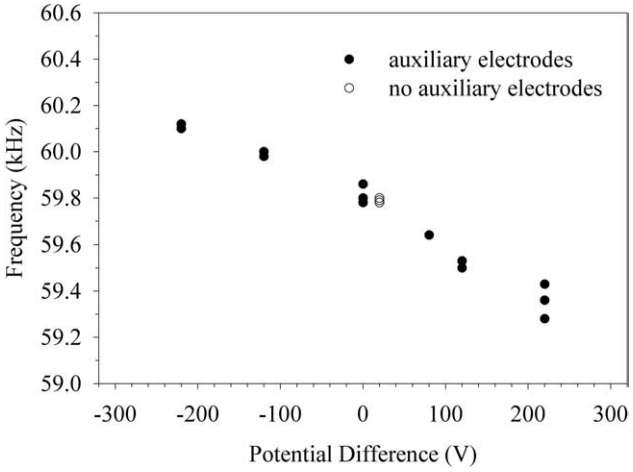

Figure 7. Plot of the resonant frequency of *m/z* = 2722 Th as a function of the applied dc potential difference to the auxiliary electrodes relative to the quadrupole rod dc offset.

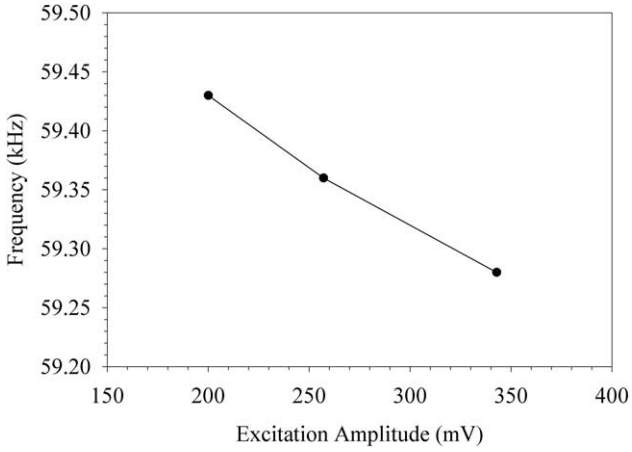

Figure 8. Plot of the resonant frequency as a function of excitation amplitude. The dc potential difference applied to the auxiliary electrodes was +220 V electrodes relative to the quadrupole rod dc offset.

tude. Plotting the resonant frequencies for a potential difference of +220 V as a function of excitation amplitude, Figure 8, reveals this dependency. The resonant frequency shifted by −150 Hz when excitation amplitude was increased from 200 to 343 mV. This can be interpreted as a decrease in the ions' secular frequency as the ion was excited to higher radial amplitudes.

The nature of the frequency shifts can be understood by examining the changes in the electric potential when a dc octopolar term is added. The electric potential can be approximated by eq 3.

$$V(x,y) = \left[A_0 + A_2\left(\frac{x^2 - y^2}{r_0^2}\right)\right]\left(U - V_{rf}\cos\Omega t\right) + S(x,y)\left(\frac{1}{2} - \frac{\left(x^4 - 6x^2y^2 + y^4\right)}{\left(r_0'\right)^4}\right)U_{aux} \quad (3)$$

The first set of terms on the right hand side describe the electric potential due to the constant potential and the quadrupolar term. The contributions from the higher order terms normally found in a round rod quadrupole have been excluded for simplicity in eq 3 and only become significant when the second term on the right hand side is close to or equal to zero. The second term consists of the expression for an octopole, the $n = 4$ term from eq 1, with a shielding function, S(x,y), applied to account for the shielding effects of the quadrupole rods. The dc octopole can be viewed as having the four rods of the A pole (A′ in Figure 4) located in the same planes as the quadrupole rods. The potential applied to the A′ pole is then the offset potential of the quadrupole. The four rods of the B pole (B′ in Figure 4) are located at the positions of the "T"-shaped auxiliary electrodes. Experimentally, the magnitude of the dc octopole is controlled by varying the dc potential difference between the quadrupole and the auxiliary electrodes and is the parameter U_{aux} in eq 3. The distance from the axis of the quadrupole to the auxiliary electrodes is $r_0' = 10$ mm. Without the effects of shielding it is expected that the potential at the point x,y = 0,0 should be equal to $U_{aux}/2$.

It should be noted that an expression for the shielding function S(x,y) in not so easily derived. Instead, an explanation of the frequency shifts is more easily given based upon an examination of the potential using the ion trajectory simulation program Simion 7.0. The shielding effects of the quadrupole rods can be quite dramatic. This is given in Figure 9, which shows the potential from the Simion model along the line x = 0 and x = y of Figure 4. The potential expected from the second term of eq 3 with S(x,y) equal to a constant is also shown. In both cases, V_{rf} and U_{aux} were 0 V and +220 V, respectively. At the point x,y = 0,0 the potential from the Simion model is 0.659 V and increases along the line x = y towards the auxiliary electrodes. Along the line x = 0 the potential decreases towards the quadrupole rod and becomes zero at the rod surface. In comparison, the calculated potential using a constant S(x,y) = 0.006 produces potentials that change much less significantly and begin to noticeably deviate from the modeled potential at about r = 1.5 mm. The value of S(x,y) = 0.006 was derived from the knowledge of V(x,y), U_{aux} = 220 V and eq 3 solved at the point x = 0, y = 0.

Examination of eq 3 shows that the dc octopole content will be a function of the ratio of V_{rf} to U_{aux}. It

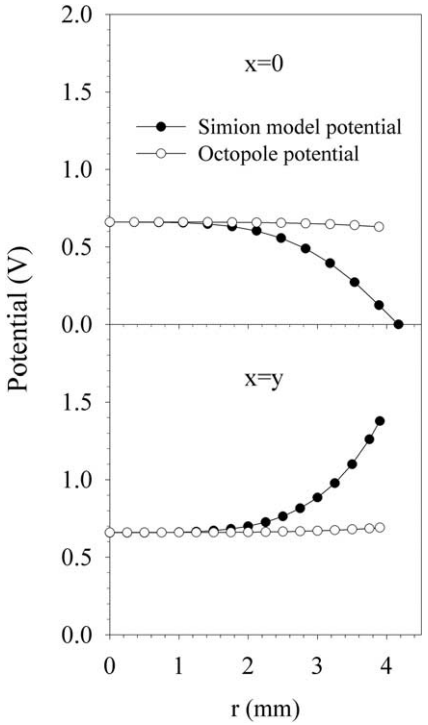

Figure 9. The potentials along the lines x = 0, towards the quadrupole rod, and x = y, towards the auxiliary electrode for both the Simion model (solid circles) and an octopole function using a constant shielding function (open circles).

Table 1. Frequency of ion motion as a function of *m/z*, V_{rf}, and U_{aux}.

m/z	V_{rf}	U_{aux}	Frequency (Hz)
2722	660.9	0	60,460
2722	660.9	220	60,270
1361	330.45	0	60,460
1361	330.45	110	60,270
1361	330.45	220	60,060

can be expected that the dc octopole content can be held constant with changing mass by keeping the ratio of V_{rf} to U_{aux} constant. This can be shown by recognizing that in the expression for the Mathieu parameter *q*, eq 4, the mass of the ion is proportional to V_{rf} when *q* is held constant and the mass is changed [19].

$$q = \frac{4eV_{RF}}{mr_0^2\,\Omega^2} \tag{4}$$

Maintaining a constant ratio of V_{rf} to U_{aux} with mass will keep the ions' fundamental frequency of motion constant. Simulations showed that decreasing *m/z* from 2722 to 1361 Th, V_{rf} from 660.9 to 330.45 V, and U_{aux} from 220 to 110 V gave ion trajectories producing identical fundamental frequencies of motion; this is shown in Table 1. In all cases the ions were started at x,y = 1.06 mm,0 mm with zero kinetic energy, no collisions and no excitation. Leaving U_{aux} at 220 V for both *m/z* = 1361 Th and *m/z* = 2722 Th results in a shift of −210 Hz. A practical implementation of the dc octopole would require that either U_{aux} is scanned with mass while the excitation frequency is held constant or that U_{aux} is held constant and the excitation frequency is scanned with mass.

Simulation Results

Collision Frequency and Available Center-of-Mass Collision Energy

Estimates of both the collision frequency and center-of-mass collision energy available for internal excitation of the ion were obtained for the round rod quadrupole LIT without the auxiliary electrodes using the ion trajectory simulator described in reference 1. A total of 100 ion trajectories were run. An excitation amplitude and frequency of 80 mV and 59,660 Hz, respectively, were employed and the trajectories were allowed to run for up to a maximum duration of 100 ms. A pressure of 3.5e-5 torr of nitrogen was used in the simulation. Out of 100 trajectories 81 reached the maximum duration allowed, those that did not resulted in trajectories that terminated upon a quadrupole rod. It was found that a collision occurred on average about once every 233 μs (a collision frequency of 4.3 kHz) with an average energy loss of 0.167 eV per collision or a total energy loss of 72 eV in 430 collisions in a 100 ms period. This compares to an average of 274 collisions and a total energy loss of 0.22 eV in 100 ms when no was excitation applied. The total energy loss is equivalent to about twice the center-of-mass collision energy. The center-of-mass collision energy is equal to the maximum amount of energy that could be transferred to internal energy of the ion [1].

Frequency Shift versus Auxiliary Electrode Potential

Ion trajectories were also run on the 2-D array shown in Figure 1 using the ion trajectory program Simion 7.0. The ion *m/z* = 2722 Th was started at different radial amplitudes along the line x = 0. The ion was given zero kinetic energy and no collisions were allowed. This produced motion along the line x = 0 only. Data were recorded for the position of the ion every microsecond for a total of 25 ms. The trajectory was then fast-Fourier-transformed to obtain the fundamental frequency of the ions' motion [20]. The trajectories were then analyzed to obtain the maximum radial amplitude that the ion reached during the course of the simulation. The fundamental frequency was plotted as a function of the maximum radial amplitude attained. This was carried out for a range of potentials applied to the auxiliary electrodes. The data are presented in Figure 10. The data shows that when a positive potential was applied to the auxiliary electrodes, the frequency shifted downwards. When a negative potential was applied, an upward shift in frequency was observed. When the potential difference was zero, a negative shift in frequency was observed at higher radial amplitude but the magnitude of this shift was significantly less than when the potential was non-zero, particularly when r_{max} was

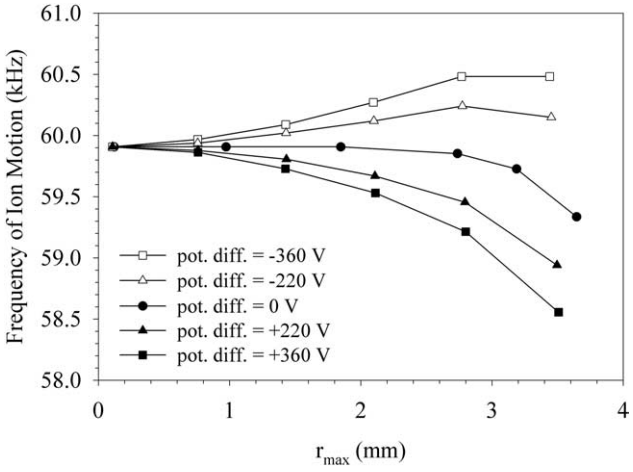

Figure 10. Frequency of ion motion along the x = 0 vector of the electrode array shown in Figure 1. The frequency of motion was obtained by fast Fourier transforming the 25 ms ion trajectory used in the simulation. The data were plotted against the dc potential difference applied to the auxiliary electrodes and the maximum radial amplitude that the ion sampled during the trajectory.

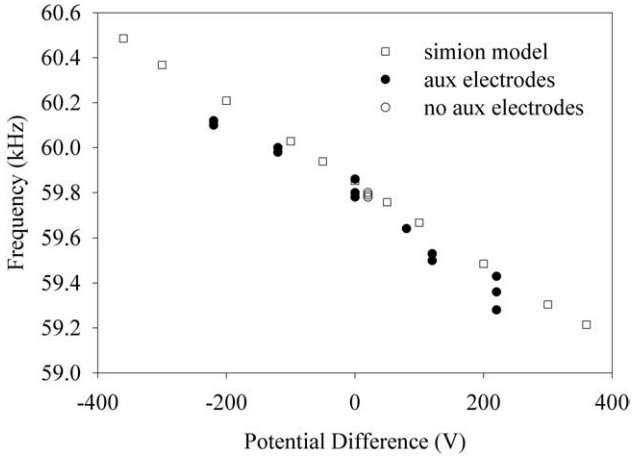

Figure 11. Experimental (solid and open circles) resonant frequencies and the resonant frequencies derived from simulations (open squares) as a function of dc potential difference between the auxiliary electrodes and the quadrupole rod offset. The frequencies derived from the simulations are from ion trajectories whose maximum radial amplitude was ≈2.8 mm. The open circles represent data obtained from a quadrupole without any auxiliary electrodes.

less than about 3 mm. In Figure 11, secular frequencies have been plotted as a function of the potential on the auxiliary electrodes, when r_{max} ≈ 2.8 mm. Figure 11 shows the same trend as the experimental data. It should be noted that the fundamental frequencies obtained from the model have been corrected for the difference in r_0 between the model and the real quadrupole. At low q values (<0.4) the fundamental angular frequency w_0 in a quadrupolar field can be estimated using [31],

$$\omega_0 = \beta \frac{\Omega}{2} \approx q \frac{\Omega}{\sqrt{8}} = \frac{4eV}{m\Omega^2 r_0^2} \frac{\Omega}{\sqrt{8}} \quad (5)$$

The fundamental frequency is inversely proportional to the square of r_0. This leads to a correction factor of 0.989953 (r_0(model)^2/r_0(real)^2 = 4.149^2/4.17^2). The frequencies obtained from the model were multiplied by this factor.

The correlation of the simulation data with the experimental data is quite good. Had the simulation data been obtained for a lower value of r_{max}, the frequency shifts would have been reduced. The similarity of Figures 7a and 11 suggests that ions were attaining radial amplitudes about 2.8 mm experimentally.

The direction of the frequency shifts can be understood by examining the potentials along the lines x = 0 and x = y in the array of Figure 3. Figure 12 shows the pseudo-potential well for mass 2722 Da, and the effects of the potentials from the auxiliary electrodes including the shielding by the quadrupole rods. The potentials of Figure 12 were calculated by summing the calculated pseudo-potential with the measured static potential from the Simion model.

The expression for the pseudo-potential as a function of x and y is given by

$$V_{eff}(x,y) = \frac{qV_{rf}}{4}\left(\frac{x^2+y^2}{r_0^2}\right) \quad (6)$$

where q = 0.205, V_{rf} = 660.9 V, and r_0 = 4.149 mm [2, 6]. Eq 4 is for a pure quadrupolar field with no contributions from higher order fields. Calculation of the effective potential including the non-zero contributions from the higher order terms changes the effective potential slightly at high radial amplitudes. Omission of the higher order terms does not affect the following qualitative discussion on the effects of the dc octopolar field on the ions' secular frequency.

The static potential was extracted from the Simion model with the potentials on the quadrupole rods set to 0 V. This was done for both +220 and −220 V applied to the auxiliary electrodes. The sum of the pseudo-potential and the static potential produced an expected

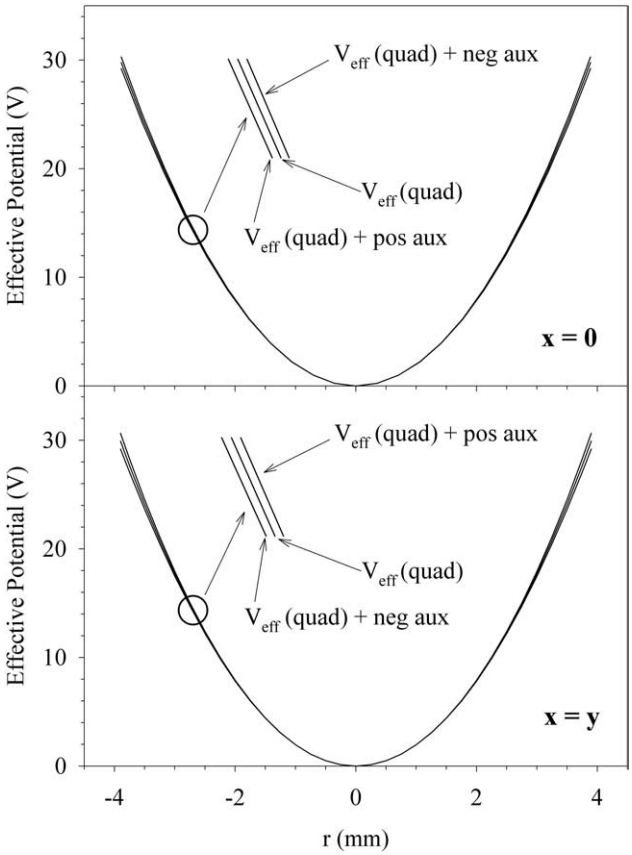

Figure 12. This figure shows the shape and depth of the pseudo potential well and the effects on the pseudo potential when a positive or negative potential is applied to the auxiliary electrodes. Applying a negative potential produces a narrower or deeper well along the x = 0 vector of Figure 3. Along the x = y vector the well becomes shallower when a negative potential is applied to the auxiliary electrodes. The opposite effect is observed when the applied potential is positive, a deepening of the well along the x = y vector and a shallower well along the x = 0 vector.

offset at the bottom of the potential well [13]. In practice the ions are cooled to the bottom of the potential well before excitation and are unaffected by the offset. The secular frequency is dependent upon the depth and shape of the potential well and not the offset. In Figure 12, the ordinates of the potentials have been offset so that bottoms of the potential wells coincide at zero. The top frame of Figure 12 shows the potentials along the line x = 0, the orientation in which the dipolar excitation is applied. A negative potential, applied to the auxiliary electrodes, causes the potential wall to rise more quickly, resulting in a deeper potential well for the same value of *r*. The opposite effect occurs when the potential applied to the auxiliary electrodes is positive: the potential well becomes shallower. The deeper well leads to an increase in the ions frequency of motion (negative potential) while the shallower well leads to a decrease in frequency (positive potential). This effect can be attributed to the shielding that the rods provide from the potentials applied to the auxiliary electrodes. The degree of shielding increases as ions approach the rods along the line x = 0.

Along the line x = y, the opposite effect occurs. Applying a negative potential to the auxiliary electrodes results in a decrease in the potential well depth, while applying a positive potential results in an increase in the depth of the potential well, as shown in the bottom frame of Figure 12.

Ion Trajectory Stability

The lack of fragmentation when a negative potential is applied to the auxiliary electrodes, shown in Figure 6, compared with the high degree of fragmentation when the potential is positive, can be understood by examining the ion trajectory during the excitation process. Three sample ion trajectories are shown in Figure 13 for potentials of 220, 0, and −220 V applied to the auxiliary electrodes. The ions' motion is separated into motion parallel to the direction of excitation, x = 0, and perpendicular to the direction of excitation. In each case, the excitation amplitude was the same as the experimental value of 255 mV. The ions were excited using the frequencies 60,100, 60,320, and 60,800 Hz for the potentials of 220, 0, and −220 V, respectively. The initial starting coordinate for the trajectories shown in Figure 13 was x,y = 0.124 mm, 0.053 mm. It should be noted that the frequencies are those inputted into the Simion model and are not corrected for the difference between the values of r_0 in the model and the real quadrupole. In the case of the positive potential, the ion trajectory continued until the time limit of 25 ms was reached. The trajectory took on a bead-like pattern with high radial amplitude in the direction parallel to the excitation. The radial amplitude that the ion attained perpendicular to the direction of excitation remained low. The ion trajectory obtained with a zero potential applied to the auxiliary electrodes showed a linear increase in radial amplitude in the direction of excitation until the trajectory terminated upon a rod surface. This occurred on a relatively short time scale, ≈1.7 ms. Examination of the ion trajectory with a negative potential applied to the auxiliary electrodes showed that the ions' radial amplitude increased linearly until the radial amplitude approached 4 mm. At this point the dc octopolar field begins to cause the ions' motion to shift out of phase with the excitation signal and coupling into motion perpendicular to the direction of excitation becomes evident. An increase in the ions' amplitude perpendicular to the direction of excitation preceded the termination of the trajectory upon a quadrupole rod. This occurred on a relatively short time scale, ≈1.7 ms. The reason for the gain in amplitude, perpendicular to the excitation vector, can be understood by examining how the static potential provided by the auxiliary

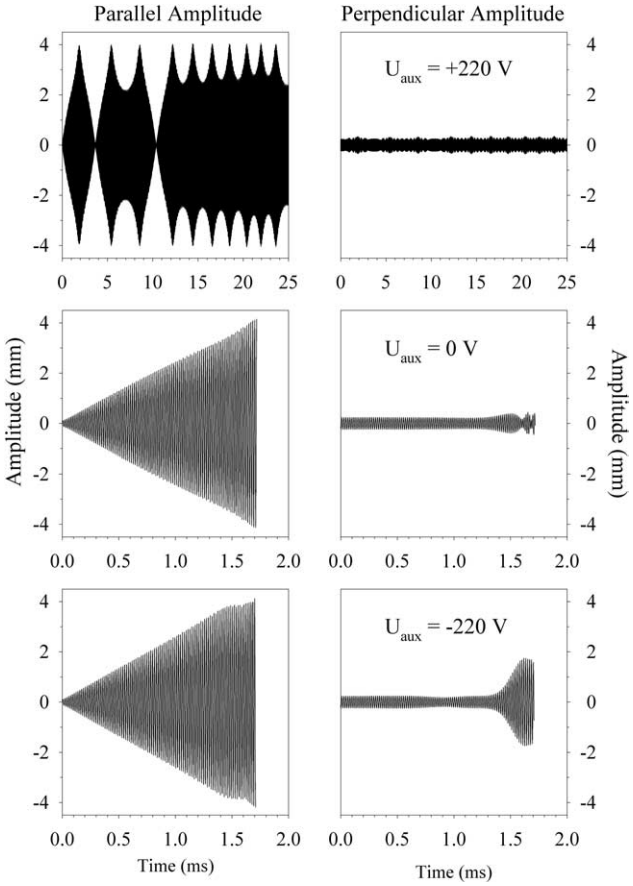

Figure 13. Representative ion trajectories are shown for when the potential applied to the auxiliary electrodes is positive (U_{aux} = +220 V), zero (U_{aux} = 0 V), and negative (U_{aux} = −220 V). An excitation amplitude of 255 mV was used in the simulations. The left hand frames show the amplitude of motion parallel to the excitation vector (x = 0), the right hand frames show the amplitude of motion perpendicular to the direction of excitation. With U_{aux} = +220 V the ion trajectory was terminated when the time limit of 25 ms was reached. With U_{aux} = 0 V the amplitude of the ion trajectory grew linearly until it terminated upon a rod at ≈1.7 ms. With U_{aux} = −220 V the ion trajectory terminated after ≈1.7 ms when the amplitude of motion perpendicular to the direction of excitation became large and the trajectory terminated upon a rod.

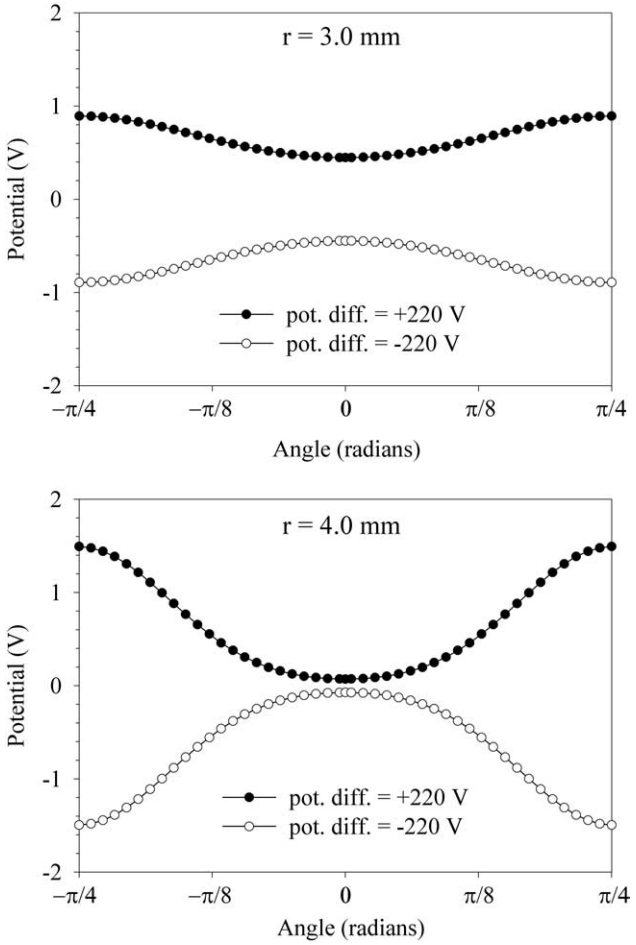

Figure 14. The lower frame shows the dc potential at a radial amplitude of 4.0 mm for potential differences between the auxiliary electrodes and the quadrupole rod offset of +220 V and −220 V as a function of angle. The upper frame shows the dc potential at a radial amplitude of 3.0 mm. In each case the rf and dc potentials applied to the quadrupole rods was 0 V. At the higher radial amplitude the shape of the potential, with +220 V applied to the auxiliary electrodes, helps to confine the ions to the region around $\theta = 0$. When the applied potential is −220 V the shape of the potential causes the ions to move away from the $\theta = 0$ region. The effect is less dramatic at lower radial amplitudes (upper frame, r = 3.0 mm) where the shape of the potential is not so distorted as a function of angle.

electrodes changed the shape of the potential well. Figure 14 shows the static potential at fixed radii as the point of interest is rotated from $\theta = -\pi/4$ to $\theta = \pi/4$. Data is shown for radii of 3 and 4 mm. The quadrupole rod is located at $\theta = 0$ radians and the auxiliary electrodes are located at $\theta = -\pi/4$ and $\theta = \pi/4$ radians. The static potential produced by +220 V applied to the auxiliary electrodes is shown as the solid circles while the static potential produced by −220 V is shown as the open circles. The static potential produced by the +220 V deepens the potential well and helps to confine the motion of the ion parallel to the direction of excitation. When the static potential is negative, the potential well develops a hump at $\theta = 0$. Consequently, ions are confined less well to the direction of excitation and may gain radial amplitude perpendicular to the direction of excitation. At lower radial amplitudes, the potential well is affected less strongly and ions are diverted little from the direction of excitation.

Conclusions

The fragmentation efficiency of a heavy ion, m/z = 2722 Th, has been increased significantly through the use of a higher order field, specifically a dc octopole. The dc octopole field was created by the addition of four auxiliary electrodes situated between the quadrupole rods at a distance of 10 mm from the axis of the quadrupole. The content of the dc octopolar field could then be adjusted by varying the potential to the auxiliary electrodes. The inclusion of the dc octopolar field has been shown to cause the ions' frequency of motion to shift out of phase with the excitation signal at high radial amplitudes. This resulted in beat-like trajectories with periods of excitation and de-excitation as the ions' frequency of motion shifted in and out of phase with the auxiliary signal. This led to a reduction in the loss of ions on the quadrupole rods resulting in a high fragmentation efficiency relative to the fragmentation efficiency obtained when using a round rod quadrupole. This process allows the ion to be fragmented more efficiently while maintaining relatively short excitation periods.

Acknowledgments

The author acknowledges Jim Hager, Yves LeBlanc, Frank Londry, and Michael Guna for the many useful discussions related to this work. The author further acknowledges the critical and entertaining comments made by Frank Londry during his review of this manuscript.

References

1. Collings, B. A.; Stott, W. R.; Londry, F. A. Resonant Excitation in a Low Pressure Linear Ion Trap. *J. Am. Soc. Mass Spectrom.* **2003,** *14,* 622–634.
2. Michaud, A. L.; Frank, A. J.; Ding, C.; Douglas, D. J. Ion Excitation in a Linear Quadrupole Ion Trap with an Added Octopole Field. *J. Am. Soc. Mass Spectrom.* **2005,** *16,* 835–849.
3. Hager, J. W. A New Linear Ion Trap Mass Spectrometer. *Rapid Commun. Mass Spectrom.* **2002,** *16,* 512–526.
4. Douglas, D. J.; Glebova, T. A.; Konenkov, N. V.; Sudakov, M. Y. Spatial Harmonics of the Field in a Quadrupole Mass Filer with Circular Electrodes. *Tech. Phys.* **1999,** *44,* 1215–1219.
5. Sudakov, M.; Douglas, D. J. Linear Quadrupoles with Added Octopole Fields. *Rapid Commun. Mass Spectrom.* **2003,** *17,* 2290–2294.
6. Gerlich, D. Inhomogeneous rf Fields: A Versatile Tool for the Study of Processes with Slow Ions. In *Advances in Chemical Physics, Vol. 82*. Ng, C-Y; Baer, M., eds. John Wiley and Sons, Inc.: New York, 1992, pp 1–176.
7. Franzen, J.; Gabling, R.-H.; Heinen, G.; Weiss, G. Method for Mass Spectroscopic Examination of a Gas Mixture and Mass Spectrometer Intended for Carrying Out This Method. U.S. Patent 5, 028, 777, 1991.

8. Wang, Y.; Franzen, J.; Wanczek, K. P. The Non-linear Resonance Ion Trap. Part 2. A General Theoretical Analysis. *Int. J. Mass Spectrom. Ion Processes* **1993,** *124,* 125–144.
9. Franzen, J. Simulation Study of an Ion Cage with Superimposed Multipole Fields. *Int. J. Mass Spectrom. Ion Processes* **1991,** *106,* 63–78.
10. Franzen, J.; Wang, Y. Quadrupole Ion Trap with Switchable Multipole Fractions. U.S. Patent 5, 468, 958, 1995.
11. Franzen, J.; Wang, Y. Quadrupole Ion Trap with Switchable Multipole Fractions. U.S. Patent Re. 36, 906, 1995.
12. Londry, F.; Collings, B. A.; Stott, W. R. Fragmentation of Ions by Resonant Excitation in a Higher Order Multipole Field, Low Pressure Ion Trap. U.S. Patent Application 0189171 A1, 2003.
13. Loboda, A.; Krutchinsky, A.; Loboda, O.; McNabb, J.; Spicer, V.; Ens, W.; Standing, K. Novel LINAC II Electrode Geometry for Creating an Axial Field in a Multipole Ion Guide. *Eur. J. Mass Spectrom.* **2000,** 6, 531–536.
14. Londry, F. A.; Hager, J. W. Mass Selective Axial Ion Ejection from a Linear Quadrupole Ion Trap. *J. Am. Soc. Mass Spectrom.* **2003,** *14,* 1130–1147.
15. Flanagan, J. M. Mass Spectrometry Calibration Using Homogeneously Substituted Fluorinated Triazatriphosphorines. U.S. Patent 5,872,357, 1999.
16. Covey, T.; Douglas, D. J. Collision Cross Sections for Protein Ions. *J. Am. Soc. Mass Spectrom.* **1993,** *4,* 616–623.
17. Dahl, D. A. *Simion 3-D Version 7.0, Publication INEEL-95/0403*; Idaho National Engineering and Environmental Laboratory: Idaho Falls, Idaho, 2000.
18. Dehmelt, H. G. *Radiofrequency Spectroscopy of Stored Ions: Storage. Adv. Atom. Mol. Phys.* **1967,** *3,* 53–72.
19. Dawson, P. H. *Quadrupole Mass Spectrometry and Its Applications*; AIP Press: Woodbury, NY, 1995; pp 13–14.
20. French, A. P. *Vibrations and Waves*; W. W Norton and Company, Inc.: New York, NY, 1971; pp 189–196.